Transactions Briefs

A Classification of Current-Mode Single-Amplifier Biquads Based on a Voltage-to-Current Transformation

G. S. Moschytz and A. Carlosena

Abstract— **Using a simple and well-known voltage-to-current transformation, current-mode *active* RC filters that are amenable to IC realization can be derived from their voltage-based counterparts. Using this transformation, a classification of current-based single-amplifier biquads is introduced which is derived from a similar voltage-based classification. This classification is exhaustive in that it includes all possible current-based single-amplifier biquads.**

I. Introduction

Whereas active RC filters, based on controlled voltage sources as the active elements, are difficult to realize in IC form, filters based on current amplifiers appear to hold far more promise [1]. This is because both current gain devices, and resistors based on transistor transconductance, can be well controlled in an IC environment. Rather than reinvent new current-mode filter circuits, it has been previously shown that voltage-based circuits can readily be transformed into current-based circuits using a network operation called *transposition* [2], [3]. The two dual (i.e. voltage-based and current-based) circuits have also been shown to be related to the concepts of a network and its *adjoint,* the two circuits being called *interreciprocal* [4], [5]. Most importantly, a network and its adjoint (which is the relationship between the original voltage-based circuit and its current-based counterpart) have identical sensitivities, which implies that design rules and optimization strategies that have been developed for voltage-based active filters can be directly adapted to current-based filters.

Using the transposition-based voltage-to-current transformation, it is shown in the following that the same categories of current based single-amplifier biquads (SABs) exist, as are known for voltage-based circuits. This leads to a comprehensive filter classification for current-based SABs that corresponds directly to the classification that has previously been derived for voltage-based SABs [7], [8]. Furthermore, as has already been pointed out previously [4] thanks to the transformation used, it follows that a previously optimized voltage-based filter [9] can be directly transformed into a current-mode filter without losing its optimum characteristics. This was subsequently also shown in [6]. Whereas the design of current amplifiers is still in its beginnings, various design suggestions have already been made in the literature [6] and [10].

II. Two-Port Transformation for Voltage-to-Current Transfer Function

In what follows, we briefly recapitulate the voltage-to-current transformation introduced in [2]–[3] as a dual transposition, which was also shown in [4] to be based on the adjoint network concept. Consider the passive RC two-port shown in fig. 1a. In terms of the short-circuit admittance parameters, it readily follows that the open circuit voltage transfer function is given by

$$\hat{t}_{12} = \left.\frac{V_2}{V_1}\right|_{I_2=0} = -\frac{y_{21}}{y_{22}} \tag{1}$$

where "^" denotes passivity on the part of the two-port. Consider now the same RC two-port, but driven from a current source at the output terminal 2 and short-circuited at the input terminal, as shown in fig. 1b. The short-circuit current transfer function results as:

$$\hat{s}_{21} = \frac{-I_1}{I_2} = -\frac{y_{12}}{y_{22}} \tag{2}$$

Since the two-port is passive, it follows that $y_{12} = y_{21}$, so that:

$$\hat{t}_{12}(s) = \hat{s}_{21} = -\frac{y_{12}}{y_{22}} \tag{3}$$

According to [2] and [3], the circuit of fig. 1b is the transpose of the circuit in fig. 1a.

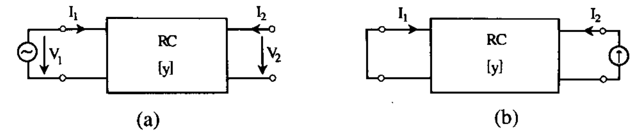

Fig. 1. Passive RC network a) voltage transfer, b) current transfer.

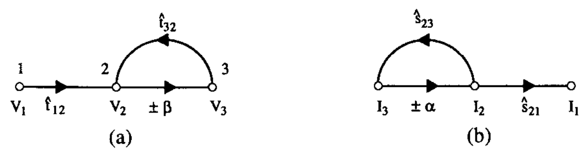

Fig. 2. Basic signal-flow graph a) for voltage-based biquad, b) for curent-based biquad.

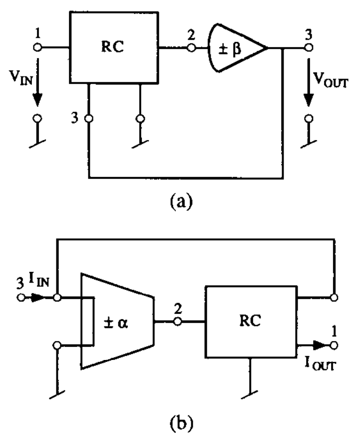

Fig. 3. Block diagram corresponding to sfg in fig. 2: a) voltage-based biquad, b) current-based biquad.

Manuscript received May 15, 1992; revised manuscript received May 15, 1993. This paper was recommended by the Associate Editor D. J. Allstot.

The authors are with the Institute for Signal and Information Proc., Swiss Federal Institute of Technology, ETH Zurich, CH-8092, Zurich, Switzerland.

IEEE Log Number 9215086.

TABLE I FOUR CLASSES OF SINGLE-AMPLIFIER BIQUADS BASED ON FEEDBACK FUNCTION $t_{32}(s)$

Class	Feedback Configurations	Root Locus of Closed-Loop Poles	Feedback Function $t_{32}(s)$	Filter Examples
1	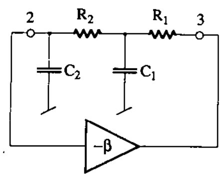 Lowpass in Feedback Loop	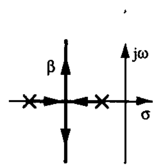	$k_{32}\frac{\omega_0^2}{s^2+\frac{\omega_0}{\hat q}s+\omega_0^2}$ $\omega_p=\omega_0\sqrt{1+k_{32}\beta}$ $q_p=\hat q\sqrt{1+k_{32}\beta}$	1. Bandpass 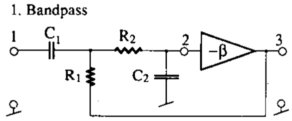 2. Lowpass 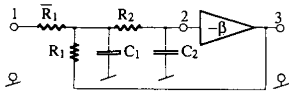
2	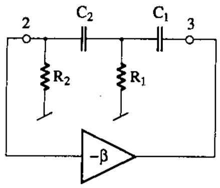 Highpass in Feedback Loop	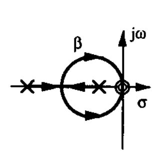	$k_{32}\frac{s^2}{s^2+\frac{\omega_0}{\hat q}s+\omega_0^2}$ $\omega_p=\frac{\omega_0}{\sqrt{1+k_{32}\beta}}$ $q_p=\hat q\sqrt{1+k_{32}\beta}$	1. Bandpass 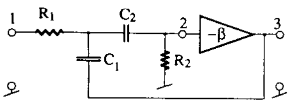 2. Highpass 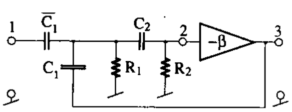

TABLE I: CONTINUED

	Feedback Configuration	Root Locus of Closed-Loop Poles	Feedback Function $t_{32}(s)$	Circuit Examples
3	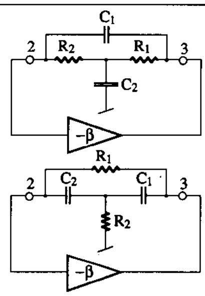	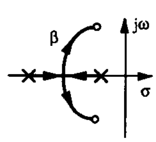 Bandrejection in Feedback Loop	$k_{32}\frac{s^2+\frac{\omega_z}{q_z}s+\omega_z^2}{s^2+\frac{\omega_0}{\hat q}s+\omega_0^2}$ $\omega_p=\omega_0\left[\frac{1+k_{32}\beta\left(\frac{\omega_z}{\omega_0}\right)^2}{1+k_{32}\beta}\right]^{1/2}$ For $\omega_z=\omega_0$: $\omega_p=\omega_z$ $q_p=\hat q\frac{1+k_{32}\beta}{1+k_{32}\beta v}$ where $v=\hat q/q_z$	1. Bandpass 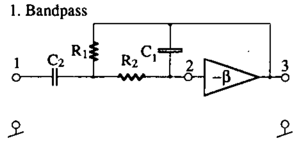 2. Lowpass 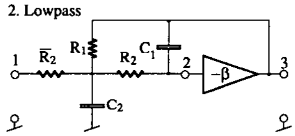 (Also possible : Highpass)
4	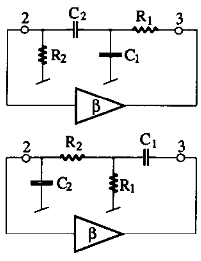	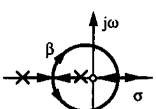 Bandpass in Feedback Loop	$\omega_k\frac{s}{s^2+\frac{\omega_0}{\hat q}s+\omega_0^2}$ $\omega_p=\omega_0$ $q_p=\frac{\hat q}{1-\frac{\omega_k}{\omega_0}\beta\hat q}$	1. Highpass 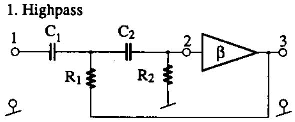 2. Lowpass 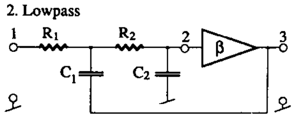 (Also possible : Bandpass, Bandreject)

Note: The parameters $\omega_0, \hat q$, k_{32}, ω_z, q_z are functions of the resistors and capacitors of the RC network used in the corresponding filter circuit.

III. A CLASSIFICATION OF SINGLE-AMPLIFIER BIQUADS

A classification of voltage-based single-amplifier biquads was introduced in [7] and expanded to include all SABs in [8]. It is based on a topology whose signal-flow graph (sfg) is shown in fig. 2a. The four possible fundamental filter classes resulting from this classification are shown in Table I. The first three classes require a negative, the fourth a positive voltage amplifier. The feedback functions $\hat t_{32}(s)$ are lowpass, highpass, bandreject and bandpass, respectively, and are realized by RC networks. The forward transfer functions $\hat t_{12}(s)$ determine the filter type. Thus, classes three and four with a bandreject and bandpass network, respectively, in the feedback path, may realize any kind of biquad filter function (other than allpass) by using an appropriate forward-path function $\hat t_{12}(s)$.

Inverting the path directions of the sfg in fig. 2a, using a positive or negative current amplifier with gain $\pm\alpha$, and reversing the operation of each $\hat t_{ij}(s)$ RC two-port as in fig. 1b such that the condition of (3) holds, we obtain the sfg of fig. 2b. This is the transposed version of the sfg of fig. 2a. The transfer function of the two are the same, although the former is based on a voltage, the second on a current amplifier. Thus, where the overall voltage transfer function for fig. 2a is:

$$T(s)=\frac{V_3}{V_1}=\pm\beta\frac{\hat t_{12}(s)}{1\mp\beta\hat t_{32}(s)} \tag{4}$$

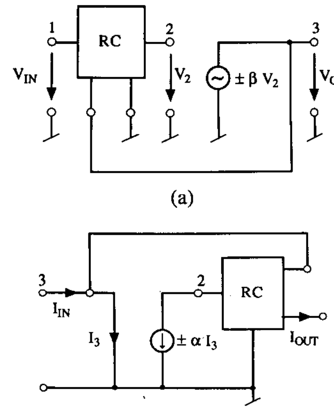

Fig. 4. a) Voltage-based biquad with voltage-controlled voltage source (VVS), b) current-based biquad with current-controlled current source (CCS).

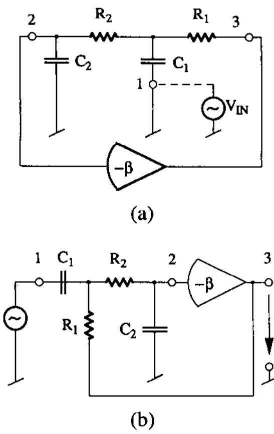

Fig. 5. Voltage-based type I single-feedback class-1 bandpass filter a) feedback configuration, b) conventional input-output configuration.

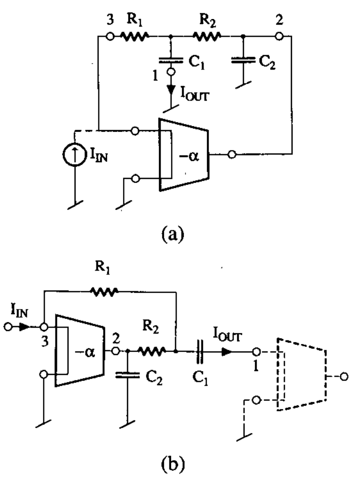

Fig. 6. Current-based type I single-feedback class-1 bandpass filter a) feedback configuration b) conventional input-output configuration.

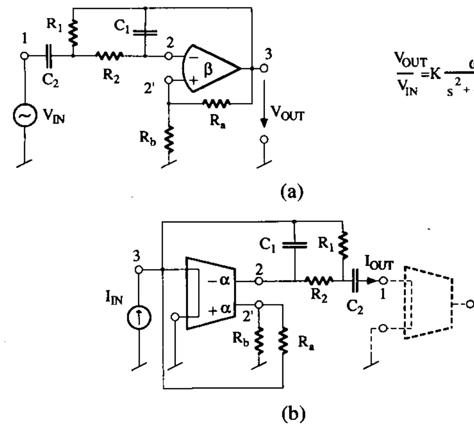

Fig. 7. Type I dual-feedback class-3 bandpass filter a) voltage-based b) current-based.

$$\frac{V_{OUT}}{V_{IN}} = K\frac{\omega_p s}{s^2 + \frac{\omega_p}{q_p}s + \omega_p^2} = \frac{I_{OUT}}{I_{IN}}$$

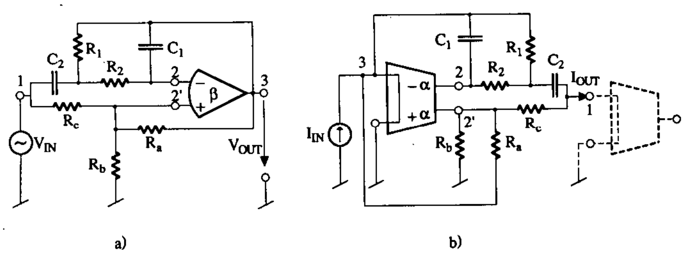

$$\frac{V_{OUT}}{V_{IN}} = K\frac{s^2 - \frac{\omega_0}{q_0}s + \omega_0^2}{s^2 + \frac{\omega_0}{q_0}s + \omega_0^2} = \frac{I_{OUT}}{I_{IN}}$$

Fig. 8. Type II dual-feedback class-3 allpass filter a) voltage-based b) current-based.

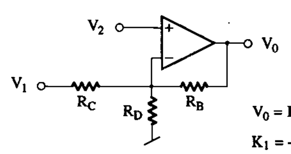

$$V_0 = K_1V_1 + K_2V_2$$
$$K_1 = -\frac{R_B}{R_C} \quad K_2 = 1 + \frac{R_B}{R_C} + \frac{R_B}{R_D}$$

Fig. 9. Dual-input signal-output voltage amplifier.

the overall current transfer function for the sfg of fig. 2b is

$$I(s) = \frac{I_1}{I_3} = \pm\alpha\frac{\hat{s}_{21}(s)}{1 \mp \alpha\hat{s}_{23}(s)}\Bigg| = T(s) \qquad (5)$$
$$\alpha = \beta$$
$$\hat{s}_{21} = \hat{t}_{12}$$
$$\hat{s}_{23} = \hat{t}_{32}$$

The block diagrams corresponding to the sfg's of fig. 2 are shown in fig. 3a and b, the corresponding controlled source representations in fig. 4a and b.

In ([7], p. 133) and [8], the voltage-based networks corresponding to the topology shown in Figs. 2a, 3a, and 4a are called single-ended input (or type I), single-feedback networks. Depending on whether the feedback function $\hat{t}_{32}(s)$ corresponds to that of a lowpass, highpass, bandreject, or bandpass filter, the corresponding class is one, two, three, or four, respectively. Class one to three networks have negative feedback (i.e. $-\beta$), class four positive feedback (i.e. $+\beta$). Consider, for example, the I-SF-1, i.e. type I (or single-ended input) single-feedback, class one (or "low-pass-in-the-feedback-loop") bandpass filter shown in fig. 5a. The voltage transfer function from terminal three to two, i.e. $\hat{t}_{32}(s)$, is that of a lowpass filter (i.e. class one filter). Driving the network from a voltage source V_1 connected to terminal one does not, in the ideal case, effect $\hat{t}_{32}(s)$, while providing a forward-path voltage transfer function $\hat{t}_{12}(s)$ corresponding to that of a bandpass filter. The filter, whose overall transfer function is determined by $\hat{t}_{12}(s)$, is therefore a bandpass filter. It is redrawn in the conventional input-output configuration in fig. 5b.

TABLE II CURRENT TRANSFORMED ACTIVE RC BIQUADS

Voltage-Based Biquads		Current-Based Biquads	
Feedback Configuration	Input-Output Configuration	Feedback Configuration	Input-Output Configuration
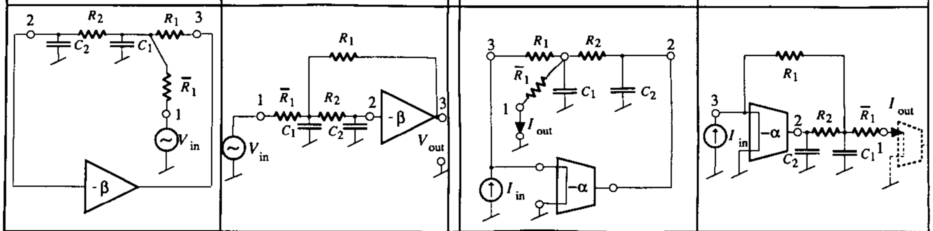			
I-SF-1 Lowpassfilter	$\frac{V_{out}}{V_{in}} = K\frac{\omega_p^2}{s^2+\frac{\omega_p}{q_p}s+\omega_p^2} = \frac{I_{out}}{I_{in}}$		
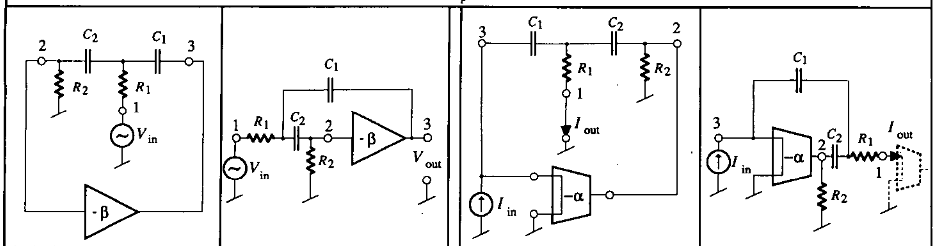			
I-SF-2 Bandpassfilter	$\frac{V_{out}}{V_{in}} = K\frac{\omega_p s}{s^2+\frac{\omega_p}{q_p}s+\omega_p^2} = \frac{I_{out}}{I_{in}}$		

TABLE II: CONTINUED

Voltage-Based Biquads		Current-Based Biquads	
Feedback Configuration	Input-Output Configuration	Feedback Configuration	Input-Output Configuration
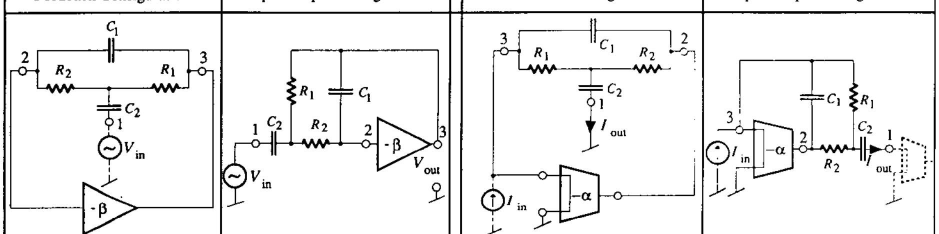			
I-SF-3 Bandpass filter	$\frac{V_{out}}{V_{in}} = K\frac{\omega_p s}{s^2+\frac{\omega_p}{q_p}s+\omega_p^2} = \frac{I_{out}}{I_{in}}$		
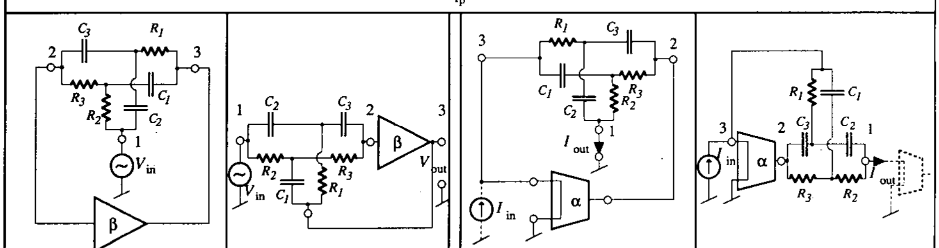			
I-SF-4 Band-rejection filter	$\frac{V_{out}}{V_{in}} = K\frac{s^2+\frac{\omega_z}{q_z}s+\omega_z^2}{s^2+\frac{\omega_p}{q_p}s+\omega_p^2} = \frac{I_{out}}{I_{in}}$		

Consider, now, the current transformed version of fig. 5a as shown in fig. 6a. Here the feedback current transfer function from terminal two to three, i.e. $\hat{s}_{23}(s)$ is that of a lowpass filter. Driving the network from an ideal current source I_{IN} connected to terminal three does not, in the ideal case, effect $\hat{s}_{23}(s)$, while it provides a forward-path current transfer function $\hat{s}_{21}(s)$ from terminal two to terminal one corresponding to that of a bandpass filter. The corresponding overall bandpass filter is redrawn in conventional form in fig. 6b. Notice that a cascade of current-based SABs requires the order in which the current amplifier and RC network is interconnected to be reversed, compared to that of voltage-based SABs. Proceeding in precisely the same way, current-based SABs of the other three classes can be derived from their voltage-based counterparts, as demonstrated in Table II. Naturally, as with voltage-based SABs, there are several filter types available with each class. The most versatile are class three (in which lowpass, highpass and bandpass filter responses are readily available) and class four (which adds band-rejection and even, within limits, allpass, to those available with a class three network).

In [7] and [8], three additional basic topologies are added in the classification of SABs. The fundamental sfgs of these topologies along with their transposed version for current-mode operation are shown in Table III. The first, that of dual feedback (DF) is especially

TABLE III A CONDENSED CLASSIFICATION OF SINGLE-AMPLIFIER SECOND-ORDER ACTIVE NETWORKS: SFG REPRESENTATION

	Voltage Mode	Current Mode
1. Type I Single Feedback Class i (I - SF - i)	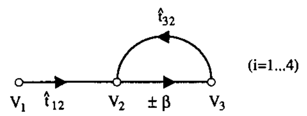	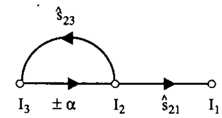
2. Type I Dual Feedback Class i (I - DF - i)	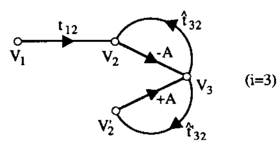	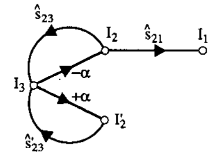
3. Type II Single Feedback Class i (II - SF - i)	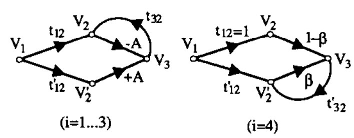	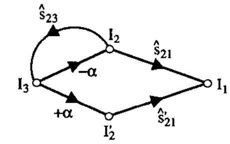
4. Type II Dual Feedback Class i (II- DF - i)	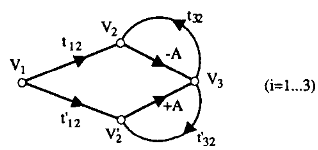	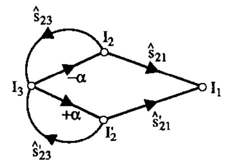

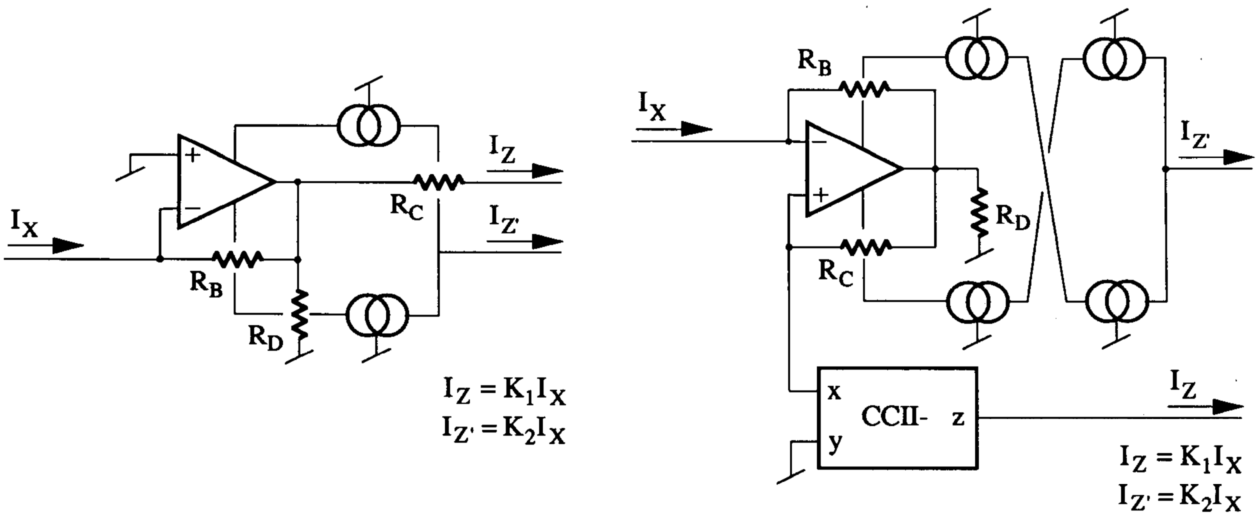

$$\text{in all cases:}\quad K_1 = -\frac{R_B}{R_C} \qquad K_2 = 1 + \frac{R_B}{R_C} + \frac{R_B}{R_D}$$

(a) (b)

Fig. 10. Possible single-input dual-output current amplifiers (based on opamps) a) first version, b) second version.

useful for class three networks. A typical voltage-based type I-dual feedback-class three (i.e., I-DF-3) bandpass network is shown in fig. 7a. The corresponding current-transformed I-DF-3 bandpass filter is shown in fig. 7b. Similarly, a voltage-based type II-dual feedback-class three allpass filter is shown in fig. 8a and the corresponding current-based II-DF-3 allpass filter in fig. 8b. Note that type II implies a topology with a differential input to the amplifier, or, in other words, a topology with two parallel forward paths of opposite polarity. Thus, the four possible basic topologies are 1) single-ended-input, single feedback or I-SF; 2) single-ended-input, dual feedback or I-DF; 3) differential input, single feedback or II-SF; and 4) differential input and dual feedback, or II-DF. The first category can be combined with the four feedback classes of Table I, the second mainly with class three, the third and fourth, within certain limits, with all four classes. More details in this regard will be published in a forthcoming paper.

The purpose of dual-feedback is to permit high-Q SABs to be designed with class-three networks using a bridged-T in the feedback loop [7]. By adding a resistive positive-feedback loop to the existing frequency-dependent negative feedback loop, the Fialkow-Gerst limitations of the zeros in the numerator of $\hat{t}_{32}(s)$ or $\hat{s}_{23}(s)$

can be overcome [7] and [8]. Furthermore, by having a differential input (output) in the voltage-based (current-based) circuit, zeros with arbitrary location in the s-plane are available. Thus, non-minimum phase SABs and, in particular, allpass networks can readily be obtained (see fig. 8).

It has been pointed out previously [4] that not only the transfer function of a current-mode filter, obtained as the adjoint of its voltage-mode version, remains unchanged, but that other important characteristics of the two will also remain unchanged. Thus, a voltage-mode circuit, optimized according to some criterion such as the minimization of the gain-sensitivity product [7], will remain optimum after the transformation into a current-mode circuit. Moreover, filter circuits, resulting from existing CAD programs and handbooks, e.g. [9], can be directly transformed into their current-mode counterparts, while retaining the same component values. Naturally, the fact that the current-mode version of the filter is more suited for on-chip realization, it will result in superior performance, once a comparison with an on-chip voltage-mode version is carried out. This has been shown, for example, in [11].

IV. Practical Considerations

It could be argued that the transformation from voltage-mode to current-mode SABs, and consequently their classification, has, as yet, little practical significance. Whereas the classical opamp is well established as the active element in the voltage domain, practical current amplifiers, as required after the transformation, do not yet exist. However, we believe that precisely because of the considerable advantages anticipated with current-mode circuits, it will not be long before current-mode amplifiers will be available. In the meantime, in order to permit a comparison to be made between current- and voltage-mode SABs, the authors have previously suggested various active devices, made up of opamps and current mirrors that can be used in current-mode SABs [6], [10]. Although their implementation cannot be considered optimal, at least they permit a laboratory comparison between current and voltage circuits to be made. A more detailed analysis, including experimental results using these circuits, can be found in the references. Here we outline only the basics of the method.

The idea behind our current-mode circuits is to isolate the opamp together with the resistive feedback loop from the voltage-mode SAB [12]. The resulting device is a dual input, single output voltage amplifier as shown in fig. 9. However, for our transformation into the current domain, a single input, dual output current amplifier is required. To obtain this, we suggest the two possible circuits shown in Figs. 10a and 10b. The first employs only two additional current mirrors, whereas the second employs an additional current conveyor (CCII-) to achieve a high impedance in both outputs. The polarity of the opamps corresponds to the positive feedback SABs and must be reversed for the negative feedback circuit, as shown in [10]. Incidentally, it should be pointed out that this approach is more versatile than that suggested in [12], because it can be applied to both positive- and negative-feedback SABs.

References

[1] C. Toumazou, F. J. Lidgey, and D. G. Haigh, "Analogue IC design: The current-mode approach," London: Peter Peregrinus Ltd., 1990.

[2] B. B. Bhattacharyya and M. N. S. Swamy, "Network transposition and its application in synthesis," *IEEE Trans. on Circuit Theory,* vol. 18, pp. 394–397, May 1971, pp. 394–397.

[3] M. N. S. Swamy, C. Bhushan, and B. B. Bhattacharyya, "Generalized dual transposition and its applications," *Journal Franklin Inst.,* vol. 301, pp. 465–476, May 1976.

[4] G. W. Roberts and A. S. Sedra, "All current-mode frequency selective circuits," *Electron. Lett.,* vol. 25, pp. 759–761, 1989.

[5] G. W. Roberts and A. S. Sedra, "Synthesizing switched-current filters by transposing the SFG of switched-capacitor filter circuits," *IEEE Trans. on Circuits and Systems,* vol. 38, no. 3, pp. 337–340, March 1991.

[6] G. S. Moschytz, A. Carlosena, and S. Porta, "Current-mode single-amplifier active RC filters," *Proc. of the Int'l Sym. on Signals, Systems and Electronics,* ISSSE'92, Paris, Sept. 1–4, 1992.

[7] G. S. Moschytz, "Linear integrated networks: Design," New York: Van Nostrand Reinhold, 1975.

[8] G. S. Moschytz, "Single-amplifier active filters: A review," *Scientia Electrica,* vol. 26, no. 1, Basel: Birkhäuser Publishing Co., 1980 (also printed as monograph), pp. 1–46.

[9] G. S. Moschytz and P. Horn, "Active filter design handbook" (including program disc), London: John Wiley, 1981.

[10] A. Carlosena, S. Porta, and G. S. Moschytz, "Current mode realization of negative-feedback SABs," *35th Midwest Symp. on Circuits and Systems,* Washington, Aug. 1992.

[11] R. Cabesa, A. Carlosena, and L. Serrano, "Multiple feedback filters revisited," ECCTD'93, Davos, Switzerland, Sept. 1993.

[12] G. W. Roberts and A. S. Sedra, "A general class of current amplifier-based biquadratic filter circuits," *IEEE Trans. on Circuits and Systems,* part, I, vol. 39, no. 4, pp. 257–263, 1992.

On the Multiphase Symmetrical Active-R Oscillators

Dan Stiurca, *Member, IEEE*

Abstract—**The need for polyphase signals arises in many applications in communications, signal processing and power electronics. The literature contains a large number of such oscillators [1]–[3]. Between these, the active-R oscillators are very attractive for monolithic realization. Unfortunately, a great discrepancy between the prediction of their linear analysis [3] and the experimental results can be observed. Therefore, a new approach for the analysis of m-phase symmetrical active-R oscillators (SARO) using standard Op Amps will be presented.**

I. Introduction

The basic stage used in SARO is the standard Op Amp inverting stage, as in fig. 1, [3]. Let us consider that the amplifier's slew rate isSR, and the gain $G = R_F/R_I$ is greater than unity. If such a stage is driven by a triangular input signalV_I of period T, amplitudeV_m and having the slopes equals to the amplifier'sSR, then the steady state output signal V_o must have the same period, and the same amplitude V_m, since there exists a relation:

$$V_m = \frac{T}{4}SR. \qquad (1)$$

The output signal will change the sign of its slope at the moment t_1, when the voltage v_N at the inverting input reaches the threshold voltage V_{TH}, fig. 2, necessary for the commutation of the Op Amps input stage [4]–[5], i.e. when

$$\frac{G-1}{G+1}V_m - \frac{G}{G+1}SRt_1 = V_{TH} \qquad (2)$$

Manuscript received November 13, 1992; revised September 21, 1993. This paper was recommended by the Associate Editor Bang-Sup Song.

Dan Stiurca is with the Electronics Dept. of the "Gh. Asachi" Technical University, Iasi, Romania.

IEEE Log Number 9214615.

1057-7130/94$04.00